Supplementary information for: Electron-phonon-dominated charge-density-wave fluctuations in $TiSe_2$ accessed by ultrafast nonequilibrium dynamics

Sotirios Fragkos,[1] Hibiki Orio,[2,*] Nina Girotto Erhardt,[3,4] Akib Jabed,[1,5] Sarath Sasi,[6] Quentin Courtade,[1] Muthu P. T. Masilamani,[2] Maximilian Ünzelmann,[2] Florian Diekmann,[7,8] Baptiste Hildebrand,[9] Dominique Descamps,[1] Stéphane Petit,[1] Fabio Boschini,[10] Ján Minár,[6] Yann Mairesse,[1] Friedrich Reinert,[2] Kai Rossnagel,[7,8] Dino Novko,[3,†] Samuel Beaulieu,[1] and Jakub Schusser[2,6,‡]

[1] *Université de Bordeaux - CNRS - CEA, CELIA, UMR5107, F33405 Talence, France*
[2] *Experimentelle Physik VII and Würzburg-Dresden Cluster of Excellence ctd.qmat, Universität Würzburg, D-97074, Würzburg, Germany*
[3] *Centre for Advanced Laser Techniques, Institute of Physics, 10000 Zagreb, Croatia*
[4] *European Theoretical Spectroscopy Facility, Institute of Condensed Matter and Nanosciences, Université catholique de Louvain, Louvain-la-Neuve, Belgium*
[5] *Institut National de la Recherche Scientifique – Énergie Matériaux Télécommunications Varennes, QC J3X 1S2, Canada*
[6] *New Technologies-Research Center, University of West Bohemia, 30614, Pilsen, Czech Republic*
[7] *Ruprecht Haensel Laboratory, Deutsches Elektronen-Synchrotron DESY, D-22607, Hamburg, Germany*
[8] *Institute of Experimental and Applied Physics, Kiel University, D-24098, Kiel, Germany*
[9] *University of Fribourg and Fribourg Centre for Nanomaterials, Chemin du Musée 3, CH-1700 Fribourg, Switzerland*
[10] *Advanced Laser Light Source, Institut National de la Recherche Scientifique, Varennes QC J3X 1S2 Canada*

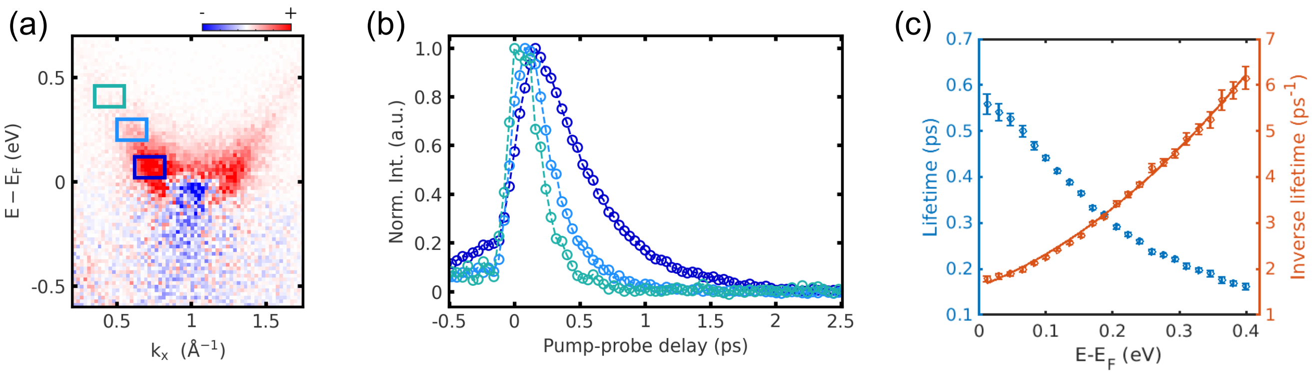

Supplementary Figure 1. (a) Differential energy-momentum cut near M with several regions of interest (ROI) boxes. The red and blue intensities denote the contrast between the pre-pump (integrated from -880 fs to -720 fs) and pump-probe overlap (integrated from -80 fs to 80 fs). (b) Intensity dynamics within each ROI, illustrating the faster decay of photoexcited electrons at higher energies. (c) Momentum-integrated electron population lifetime and corresponding inverse lifetime as a function of $E - E_F$.

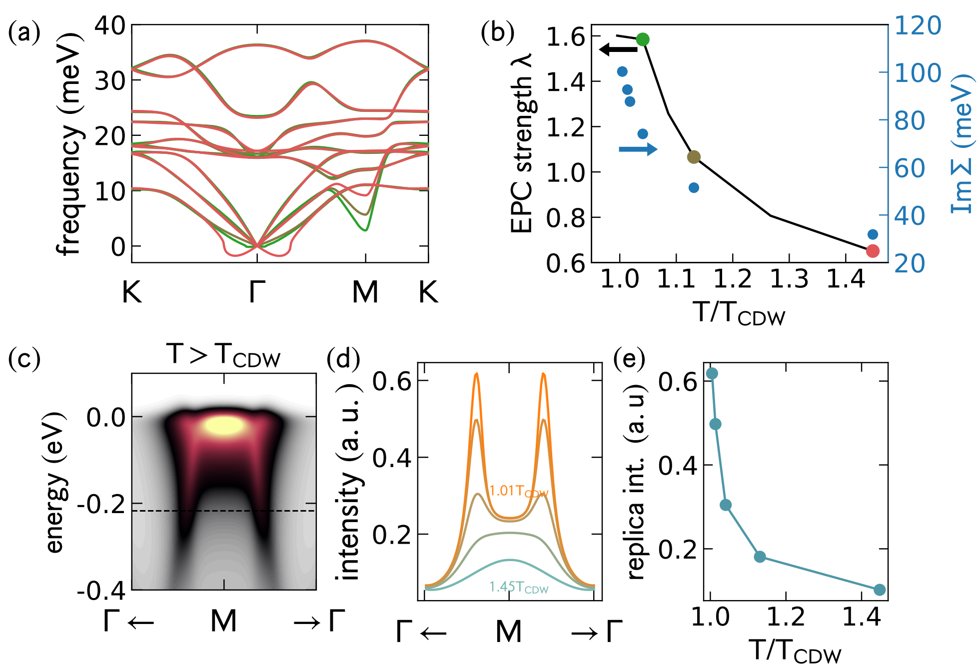

Supplementary Figure 2. (a) Phonon band structure of non-distorted $TiSe_2$ along the high-symmetry points and for several temperatures above the T_{CDW}, i.e., for 1150 K, 1300 K, and 1600 K. Note that this is done within the harmonic approximation for which $T_{\mathrm{CDW}} \approx 1100$ K. Also, note the hardening of the CDW-related acoustic phonon at the M point. (b) The calculated total electron-phonon coupling (EPC) strength λ for each temperature above T_{CDW}. The right axis shows the values for the imaginary part of the electron self-energy due to EPC (i.e., electron scattering rate), averaged over the states around the Fermi level. (c) Fluctuating replica at the M point for temperatures above T_{CDW} as obtained from the dynamical EPC scatterings. (d) The corresponding intensity of the fluctuating CDW replica coming from dynamical EPC as a function of temperature and along the M point. (e) The intensity of the replica is decreasing as a function of temperature. Note the connection between the hardening of the M acoustic phonon, the weaking of the EPC strength, and quenching of the CDW fluctuating replica as a function of increasing temperature.

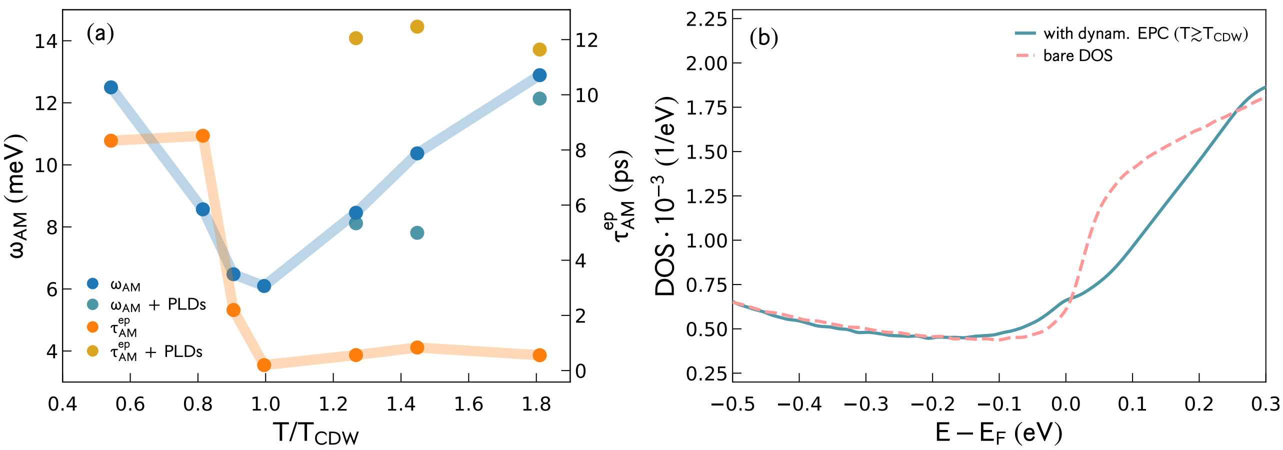

Supplementary Figure 3. (a) Frequency (blue) and lifetime (orange) of the CDW amplitude mode calculated from DFPT. We also show the corresponding results where small periodic lattice distortions are introduced also for $T > T_{\mathrm{CDW}}$ to mimic the CDW fluctuations. (b) Density of states for the bare $\mathrm{TiSe_2}$ electronic structure, as well as when the dynamical electron-phonon scatterings are included for $T > T_{\mathrm{CDW}}$. The opening of the pseudogap is evident for the latter.

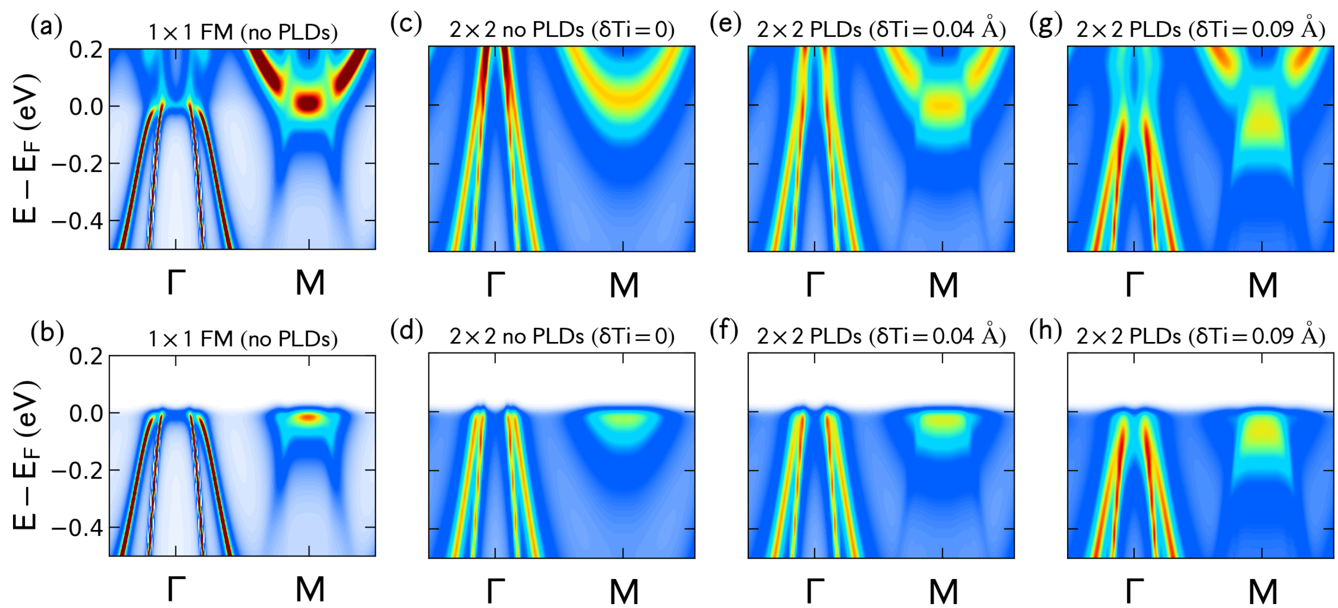

Supplementary Figure 4. (a)-(b) Electron spectral function of 1T-$\mathrm{TiSe_2}$ with dynamical electron-phonon interaction included via Fan-Migdal self-energy (FM) for temperature just above the CDW transition temperature $T \gtrsim T_{\mathrm{CDW}}$. These calculations are done for 1×1 unit cell with no periodic lattice distortions (PLDs). (c)-(h) The band structures of the 2×2 CDW phase with various values of PLDs mapped to the 1×1 unit cell. In these calculations we do not include the FM self-energy. The lower panels are equivalent to the plots in the upper panels, but weighted with the Fermi-Dirac distribution function. The comparison between the results of 1×1 band structure with FM self-energy and 2×2 result with PLDs shows that the dynamical electron-phonon scattering introduces very similar modifications to the band structure as the symmetry-breaking CDW PLDs.

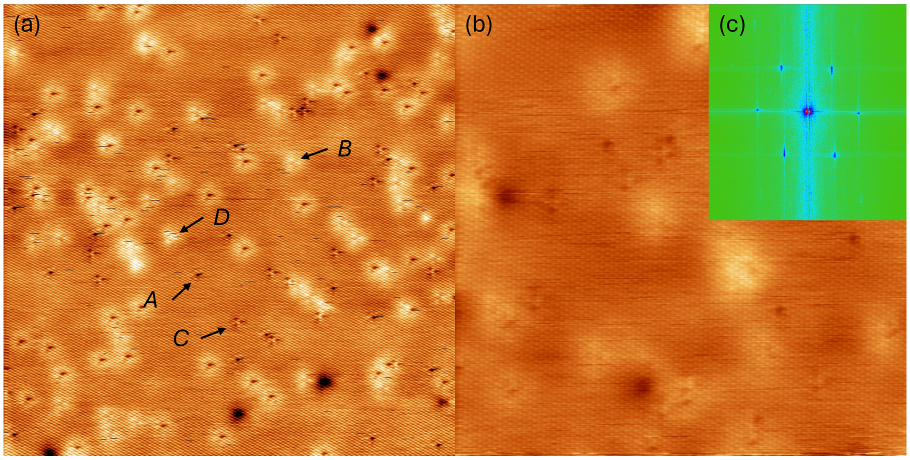

Supplementary Figure 5. To characterize the CDW fluctuations dynamics in real space and find the fingerprints of finite fluctuating periodic lattice distortions (PLD), we measured the 1T-$TiSe_2$ at RT with scanning tunneling microscopy (STM) and observed no visible signatures of the 2×2 CDW patches beyond the signal corresponding to the 1×1 unit cell charge modulation. This implies that the fluctuations likely occur at timescales below the scanning rate of the STM, further supporting our result that the localization of each CDW modulation in $TiSe_2$ at a given position is inherently dynamical, while the system as a whole is constantly in a fluctuation phase. Despite that, L and M diffusive peaks at RT were spotted in equilibrium electron diffraction measurements [1], as well as in X-ray diffuse scattering [2,3], suggesting the presence of the fluctuating PLD at RT, and possibly the appearence of the corresponding pseudogap [4]. (a) Atomically resolved empty-states STM image showing native defects (60×60 nm^2, $I_t = 1.2$ nA, $V_{\rm bias} = 0.01$ V). Different defects are labeled A, B, C, D following (PRL[5]). (b) Atomically resolved filled-states STM image (32×32 nm^2, $I_t = 0.1$ nA, $V_{\rm bias} = -0.1$ V). (c) FFT-amplitude plot from (b) showing no 2×2 CDW charge modulation associated spots.

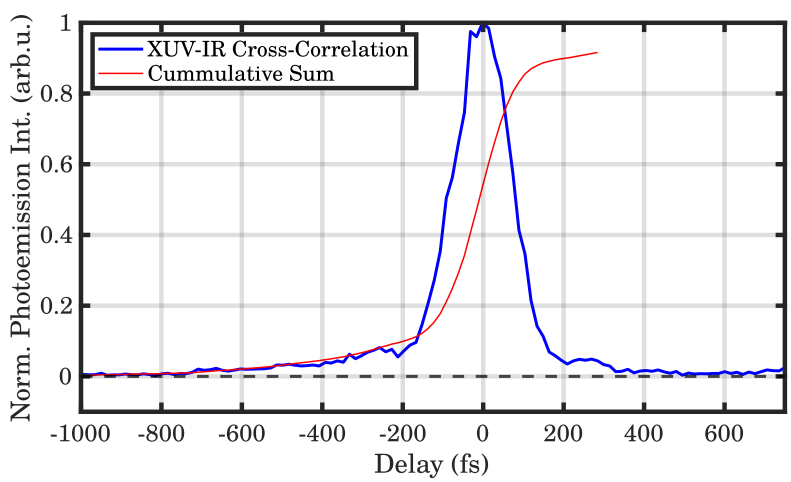

Supplementary Figure 6. **Cross-correlation between p-polarized IR pump and p-polarized XUV probe** In blue, the normalized photoemission intensity as a function of pump-probe delay, extracted for laser-assisted photoemission (LAPE) valence band replica in GeS semiconductor.

SUPPLEMENTARY REFERENCES

* hibiki.orio@uni-wuerzburg.de
† dino.novko@gmail.com
‡ schusser@ntc.zcu.cz

[1] Y. Cheng, A. Zong, J. Li, W. Xia, S. Duan, W. Zhao, Y. Li, F. Qi, J. Wu, L. Zhao, *et al.*, Nature communications **13**, 963 (2022).
[2] K. C. Woo, F. C. Brown, W. L. McMillan, R. J. Miller, M. J. Schaffman, and M. P. Sears, Phys. Rev. B **14**, 3242 (1976).
[3] X. Guo, A. Kogar, J. Henke, F. Flicker, F. de Juan, S. X. L. Sun, I. Khayr, Y. Peng, S. Lee, M. J. Krogstad, S. Rosenkranz, R. Osborn, J. P. C. Ruff, D. B. Lioi, G. Karapetrov, D. J. Campbell, J. Paglione, J. van Wezel, T. C. Chiang, and P. Abbamonte, arXiv , 2501.09968 (2025).
[4] Y. Miyahara, H. Bando, and H. Ozaki, Journal of Physics: Condensed Matter **7**, 2553 (1995).
[5] B. Hildebrand, C. Didiot, A. M. Novello, G. Monney, A. Scarfato, A. Ubaldini, H. Berger, D. R. Bowler, C. Renner, and P. Aebi, Phys. Rev. Lett. **112**, 197001 (2014).